NeuroImage 84 (2014) 27–34

Contents lists available at ScienceDirect

NeuroImage

journal homepage: www.elsevier.com/locate/ynimg

Neural correlate of resting-state functional connectivity under α2 adrenergic receptor agonist, medetomidine

Fatima A Nasrallah [a], Si Kang Lew [a], Amanda Si-Min Low [a], Kai-Hsiang Chuang [a,b,c,*]

[a] Magnetic Resonance Imaging Group, Singapore Bioimaging Consortium, Agency for Science Technology and Research, Singapore
[b] Clinical Imaging Research Centre, National University of Singapore, Singapore
[c] Department of Physiology, Yong Loo Lin School of Medicine, National University of Singapore, Singapore

ARTICLE INFO

Article history:
Accepted 5 August 2013
Available online 13 August 2013

Keywords:
Functional MRI
Resting state
Functional connectivity
Somatosensory evoked potentials
Electrophysiology
Neurovascular coupling
Adrenergic receptor

ABSTRACT

Correlative fluctuations in functional MRI (fMRI) signals across the brain at rest have been taken as a measure of functional connectivity, but the neural basis of this resting-state MRI (rsMRI) signal is not clear. Previously, we found that the α2 adrenergic agonist, medetomidine, suppressed the rsMRI correlation dose-dependently but not the stimulus evoked activation. To understand the underlying electrophysiology and neurovascular coupling, which might be altered due to the vasoconstrictive nature of medetomidine, somatosensory evoked potential (SEP) and resting electroencephalography (EEG) were measured and correlated with corresponding BOLD signals in rat brains under three dosages of medetomidine. The SEP elicited by electrical stimulation to both forepaws was unchanged regardless of medetomidine dosage, which was consistent with the BOLD activation. Identical relationship between the SEP and BOLD signal under different medetomidine dosages indicates that the neurovascular coupling was not affected. Under resting state, EEG power was the same but a depression of inter-hemispheric EEG coherence in the gamma band was observed at higher medetomidine dosage. Different from medetomidine, both resting EEG power and BOLD power and coherence were significantly suppressed with increased isoflurane level. Such reduction was likely due to suppressed neural activity as shown by diminished SEP and BOLD activation under isoflurane, suggesting different mechanisms of losing synchrony at resting-state. Even though, similarity between electrophysiology and BOLD under stimulation and resting-state implicates a tight neurovascular coupling in both medetomidine and isoflurane. Our results confirm that medetomidine does not suppress neural activity but dissociates connectivity in the somatosensory cortex. The differential effect of medetomidine and its receptor specific action supports the neuronal origin of functional connectivity and implicates the mechanism of its sedative effect.

Introduction

Spontaneous fluctuations of the blood oxygen level-dependent (BOLD) functional MRI signal at resting state enable the detection of intrinsic brain network and functional connectivity. These coherent hemodynamic fluctuations are observed in the low frequencies (<0.1 Hz) of the BOLD and CBF signals (Biswal et al., 1995; Chuang et al., 2008). While the hemodynamic footprint of such intrinsic networks has been extensively investigated, the underlying electrophysiological signature remains elusive (Laufs et al., 2003b; Leopold and Logothetis, 2003; Nir et al., 2008). Electrophysiology, which directly relates dynamic postsynaptic activity in the cerebral cortex, has been used to observe synchronization across frequency bands in large-scale functional networks. How resting-state MRI (rsMRI) recordings translate to electrophysiology readings is of uttermost interest.

Most studies to date have investigated the correlation between electroencephalogram (EEG) and the resting-state BOLD signal. The α-band activity in the occipital lobe (Goldman et al., 2002; Moosmann et al., 2003; Scheeringa et al., 2012) and frontal and parietal cortices (Laufs et al., 2003a) of human subjects negatively correlated with rsMRI at the time when global α power correlated inversely with the thalamic rate of glucose metabolism (Larson et al., 1998; Lindgren et al., 1999). Functional coupling of the regional BOLD signal and EEG oscillations in beta and gamma frequency ranges was also found in regions comprising the default mode network (DMN) and the anterior thalamic nucleus (Michels et al., 2010). Increased α and β power is related to decreased functional connectivity while gamma power positively correlated with BOLD connectivity between specific brain areas (Tagliazucchi et al., 2012). In isoflurane anesthetized non-human primates, rsMRI fluctuations were found to positively correlate with gamma-band local field potential (Shmuel and Leopold, 2008). In rodents, high correlation

* Corresponding author at: Singapore Bioimaging Consortium, 11 Biopolis Way, #02-02, Singapore 138667, Singapore. Fax: +65 64789957.
E-mail address: Chuang_Kai_Hsiang@sbic.a-star.edu.sg (K.-H. Chuang).

1053-8119/$ – see front matter © 2013 Elsevier Inc. All rights reserved.
http://dx.doi.org/10.1016/j.neuroimage.2013.08.004

between rsMRI signals and delta band oscillations under increasing α-chloralose dosages was identified (Lu et al., 2007). Ultra-slow frequency EEG signal (<0.5 Hz) was explored and found to have high regional correlations with the low-frequency BOLD signal (Pan et al., 2011). Similar correlation with ultra-slow EEG has also been reported in non-human primates, while BOLD positively correlated with the gamma power as well (He et al., 2008). In human, intracranial local field potential in interhemispheric auditory cortex showed correlation between BOLD and gamma band power (Nir et al., 2007).

Where the use of anesthesia is unavoidable in most electrophysiology and fMRI studies in animals, the choice of anesthesia and type of anesthetic used are likely to significantly affect spontaneous brain activity and neurovascular coupling. For example, a strong dependency of coherent BOLD fluctuations on isoflurane levels was seen in rats (Liu et al., 2011). Masamoto et al. showed that CBF increased with increasing isoflurane dosages while the coupling between evoked potential and CBF varied (Masamoto et al., 2009). The diverse effects of different anesthesia/sedatives and how they critically interfere with the pathway of neurovascular coupling have been well documented (Masamoto and Kanno, 2012). This could confound the interpretation of functional connectivity linking to the underlying electrophysiological mechanism.

Medetomidine, an α2-adrenergic receptor agonist, has been used as a sedative in functional connectivity MRI studies in rodents (Adamczak et al., 2010; Pawela et al., 2009; Weber et al., 2006). In previous study, we showed that medetomidine suppressed resting-state functional connectivity in receptor-dominating regions dosage-dependently but with no effect on somatosensory BOLD activation (Nasrallah et al., 2012). As a vasoconstrictor, medetomidine may affect the neurovascular coupling. To further understand the neural correlate of the medetomidine on functional connectivity, we conducted electrophysiology measurements of somatosensory evoked potential (SEP) and resting EEG under different medetomidine dosages and correlated with the BOLD signals under the same conditions. We hypothesized that the coupling between electrophysiology and BOLD signal is not changed by medetomidine and BOLD signal can reflect the underlying functional synchrony in the brain. The coupling between EEG and fMRI was further compared under a common anesthetic, isoflurane, to understand the specificity of the medetomidine effect.

Materials and methods

Animal preparation

All experiments were conducted in compliance with guidelines set forth by the institutional animal care and use committees of the Biomedical Sciences Institutes (A*STAR, Singapore). Twenty male Wistar rats weighing 300–400 g were used in the MRI study. A separate thirty male Wistar rats (300–400 g) were used in the EEG study. The rats were placed in a gas anesthesia induction chamber and 3% isoflurane was induced in a mixture of air and O_2 gases (40% O_2) via a calibrated vaporizer. Rats were maintained under 2–3% isoflurane during preparation primarily to prevent the pain response to insertion of the infusion needle, insertion of the stimulation electrodes, and scalp incision of the EEG procedure. Two types of anesthesia were used in this study, medetomidine and isoflurane.

Medetomidine

The medetomidine experiments followed the same procedure in our previous study (Nasrallah et al., 2012). Briefly, the rat received an intraperitoneal bolus of 0.05 mg/kg medetomidine (Domitor®, Pfizer, USA) after induction. An infusion line (PE50) was then inserted intraperitoneally and a continuous infusion of medetomidine via a syringe pump was started (Kd Scientific, USA) and isoflurane was switched off 10 min after the start of medetomidine infusion. Three different infusion dosages were used in separate animals: 0.1, 0.2, and 0.3 mg/kg/h (n = 5 for each dosage for fMRI; n = 8 for EEG). Data acquisition (fMRI or EEG) was started 40 min after the initiation of medetomidine infusion.

Isoflurane

After anesthetized, endotracheal intubation was performed and the rat was mechanically ventilated with a ventilator (TOPO, Kent Scientific, USA). PE-50 tubing was inserted into the tail artery for monitoring of physiological parameters and blood sampling. A 27-gauge butterfly needle was inserted into the tail vein for muscle relaxant administration. Rectal temperature was maintained at 36.5 ± 0.5 °C by a heating pad. After preparation, a bolus of 1.5 mg/kg pancuronium bromide (Sigma, Singapore) was given intravenously and isoflurane was decreased to 1.3%. Ventilation parameters were adjusted based on arterial blood pH, pCO_2 and pO_2 measures (ISTAT, Abbott, USA). Mean arterial blood pressure (MABP) and rectal temperature were continuously monitored (Model 1025, SA Instruments Inc., USA). Three different levels of isoflurane – 1.0, 2.0 and 3.0% – were investigated in the same animal (n = 5 for fMRI; n = 6 for EEG). Artificial ventilation was necessary to avoid physiological alterations with varying dosages of isoflurane so that physiology can be controlled in the normal range.

Experimental design

Medetomidine

Somatosensory evoked activation and resting-state activity were measured at three dosages of medetomidine in different animals with similar design as our previous study (Nasrallah et al., 2012). Resting-state activity was measured for 10 min using fMRI and for 5 min using EEG at 40 min after the starting of constant infusion of medetomidine. Then somatosensory evoked activation was induced by electrical stimulation of various currents and frequencies to the forepaw with a pair of electrodes inserted under the skin. For fMRI, stimulation was given to both forepaws by a block design with 60 s resting and 20 s stimulation alternately repeated three times and adding 60 s of resting at the end. For SEP study, stimulation was given to the left paw by a block design with of 30 s rest followed by 20 s stimulation. Rectangle pulses of 9 Hz frequency, 0.3 ms duration were generated by a current source (Isostim A320, World Precision Instruments, USA). Four stimulus currents – 1, 2, 3, and 4 mA – were applied with one current in each run in random order. Frequency dependent response was inspected at 3 mA and varied from 3, 5, 7, 9, to 12 Hz in random order. An additional 5 min interval was allowed in between different experimental conditions/stimuli.

Isoflurane

The somatosensory evoked activation and resting-state activity were measured under different levels of isoflurane in the same animal. Resting-state activity was measured first followed by somatosensory evoked activation. A 20 min equilibration period was allowed after switching between different levels of isoflurane to prevent cumulative effects. This is based on previous reports that the isoflurane concentration in arterial blood and brain tissue equilibrates after approximately 15 min (Antognini and Carstens, 1999; Lin, 1994). The order of isoflurane levels was randomized across animals. The same stimulus current dependent response was studied as in the medetomidine study.

MRI

All MRI measurements were performed on a 9.4 T horizontal magnet with a bore size of 31 cm diameter (Agilent Technologies, USA). The animal was then loaded into a MRI-compatible cradle (Rapid Biomedical GmbH, Germany) and its head was fixed with ear bars and a bite bar to prevent head motion. The respiration rate and pattern, and rectal temperature were monitored using a MRI compatible physiological monitoring system (Model 1025, SA Instruments Inc., USA). The rectal temperature was maintained at ~37 °C by a feedback-controlled

air heater (SA instruments Inc., USA) during the whole experiment. Two actively decoupled radiofrequency coils were used: a volume coil (7.2 cm inner diameter; Rapid Biomedical GmbH, Germany) was used for RF transmission and a custom-designed surface coil of 1.5 cm diameter positioned on the top of the animal's head as the receiver. The receiver coil was carefully positioned on top of the somatosensory area to ensure consistent B1 profile. The animal's position was adjusted based on a sagittal scout image to place the primary somatosensory cortex (SI) in the magnet center. The homogeneity of the magnetic field was optimized by using high order 3D shimming. Resting-state fMRI was acquired for 10 min (300 volumes) on ten consecutive axial slices using a single-shot spin-echo echo-planar imaging (SE EPI) sequence with TR = 2 s, TE = 45 ms, thickness = 1 mm, gap = 0.1 mm, matrix size = 64 × 64, and FOV = 25.6 × 25.6 mm^2. For fMRI of forepaw activation, 150 scans were acquired in 5 min with the same acquisition parameters. SE EPI was used because it is less biased to large vein and less susceptible to susceptibility artifacts and distortions especially at high-field.

EEG

For intracerebral EEG measurements, the rat's head was secured in a digital stereotaxic frame (Stoelting Co., USA). The skull was exposed at areas including the bregma as well as over the bilateral forelimb area in the primary somatosensory cortex (SIFL) and the regions in front of the lambdoid suture. Two holes were drilled at the left and right SIFLs (4 mm lateral and 1 m frontal to bregma) using a drill (Foredom, Romford, UK). A third hole was drilled 10 mm posterior to the right hole for the reference electrode. Drilling was performed until the surface of the dura was revealed (approximately 1 mm from the skull surface in all cases). A small opening in the dura was cut where visible blood vessels were avoided using a 27-gauge syringe needle. Then, two electrodes, fixed on a stereotaxic holder, were inserted into the cortex, 0.5–1 mm below the brain surface, which is close to cortical layer IV. Another electrode was inserted at 10 mm posterior to the right SIFL as the reference. Rectal temperature was monitored continuously via a thermometer and was maintained at 36.5 ± 0.5 °C using a heating pad.

Resting EEG and SEP were recorded under the same anesthetics and timing as the fMRI experiments. Resting EEG was recorded with a high pass filter at 0.01 Hz for 300 s (MP150, Biopac, USA). SEP was recorded under a 30 s resting followed by 20 s stimulation with a high pass filter of 0.1 Hz. The signals were amplified at a gain of 5000, sampled at 1000 Hz and recorded by software (Acknowledge, Biopac, USA) on a PC.

Data analysis

MRI

Functional MRI datasets were processed using custom-written software in Matlab (Mathworks, USA) and in C. All data was carefully checked for head movement by displaying the time series images in movie mode and calculating the center-of-mass. For SIFL activation, cross-correlation was computed by correlating the fMRI data with the box-car paradigm on a pixel-by-pixel basis with a correlation threshold >0.2 and a cluster size of 4 pixels. The three stimulation blocks were averaged into one to calculate the percentage signal change for comparison across anesthesia levels. Statistical significance was tested using ANOVA with the Bonferroni test for multiple comparisons. $p < 0.05$ was regarded as significant.

To obtain functional connectivity map, resting-state BOLD data was pre-processed by high-pass filtering at 0.01 Hz and low-pass filtering at 0.1 Hz. The 0.1 Hz cutoff was only used in generating the correlation maps. The average signals from the ventricles were regressed out to reduce contributions from physiological noise and the data was spatially smoothed with a full width at half maximum (FWHM) kernel of 1 pixel. The somatosensory connectivity map was calculated by correlation analysis based on the time-course of a 2 × 2 pixel ROI from the left SIFL region, defined by the activation map under 4 mA stimulation and by consultation with the rat brain atlas (Paxinos and Watson, 1995). A correlation coefficient higher than 0.25 was considered significant and clusters smaller than 4 pixels were rejected.

The inter-hemispheric connectivity between the left and the right SIFLs was then calculated from the entire functionally defined regions based on the activation map and the brain atlas. Even with the use of SE-EPI at high-field, BOLD signal from large vessels near the surface of the brain is still prominent. Therefore, caution was taken when defining the ROIs to avoid large vein artifact. For this analysis, similar data preprocessing was applied as described in the previous paragraph except the low-pass filter so that higher frequency could be taken into account. The time-courses from each of the ROI were then extracted without applying any threshold to calculate the correlation coefficient, coherence and power spectra. Coherence was defined as:

$$Cxy(f) = Pxy^2/Pxx \cdot Pyy \quad (1)$$

where x and y are the two input signals and Pxx and Pyy are the power spectral densities of x and y, respectively, and Pxy is the cross power spectral densities of x and y. This was computed using the 'mscohere' function with Welch's periodogram averaging method in Matlab. The average coherence in the three frequency bands: 0.01–0.04, 0.04–0.07, 0.07–0.1, 0.1–0.18, and 0.18–0.25 Hz were calculated. Power spectral density of the resting fMRI was calculated using the periodogram spectral estimation method. The total power between 0.01 and 0.25 Hz was calculated.

EEG

SEP was calculated by averaging the first 20 epochs. The integral of the absolute amplitude of the entire evoked response was calculated. Power spectral estimation of the resting EEG signal was obtained by using the periodogram method with a sampling frequency of 1000 Hz and low-pass filtered at 49 Hz. Coherence analysis was also applied to the resting EEG data from the two SIFL regions. The mean (or total) power spectral density and the mean coherence within 5 predefined frequency bands based on EEG conventions (δ, 1–4 Hz; θ, 4–8 Hz; α, 8–13 Hz; β, 13–30 Hz; γL, 30–45 Hz) were calculated. Typical gamma band is in the range of 30–150 Hz. In this study, only the low gamma band (γL) was analyzed because less contribution is expected from the high gamma band as the power is much lower (Lu et al., 2007). Relative power distribution within each frequency band was obtained by normalizing by the total power between 1 and 45 Hz. Statistical significance was tested using ANOVA with the Bonferroni test for multiple comparisons. $p < 0.05$ was regarded as significant.

Results

BOLD activation and SEP under medetomidine

Consistent SEPs were obtained in the contralateral S1FL cortex following a stimulation of 3 mA with a range of frequencies from 3, 5, 7, 9, to 12 Hz. Fig. 1 shows the stimulus frequency dependent SEPs at 0.1, 0.2 and 0.3 mg/kg/h of medetomidine. Average SEP under 0.1 and 0.3 mg/kg/h medetomidine showed similar responses with no significant difference in the peak amplitude or total interval at the same stimulus frequency (Figs. 1a and b). Highest SEP integrals were seen between 3 and 7 Hz. No significant difference was observed across any dosages of medetomidine (Fig. 1c).

Robust BOLD activations were detected in SIFL with stimulus currents varied from 1 to 4 mA. Fig. 2a represents the time courses of BOLD activation following 9 Hz and 3 mA stimuli at different medetomidine doses. The percent signal change of BOLD activation was the same across the dosages. Fig. 2b shows the averaged SEPs under the same stimuli. The peak amplitude of 9 Hz stimulus was

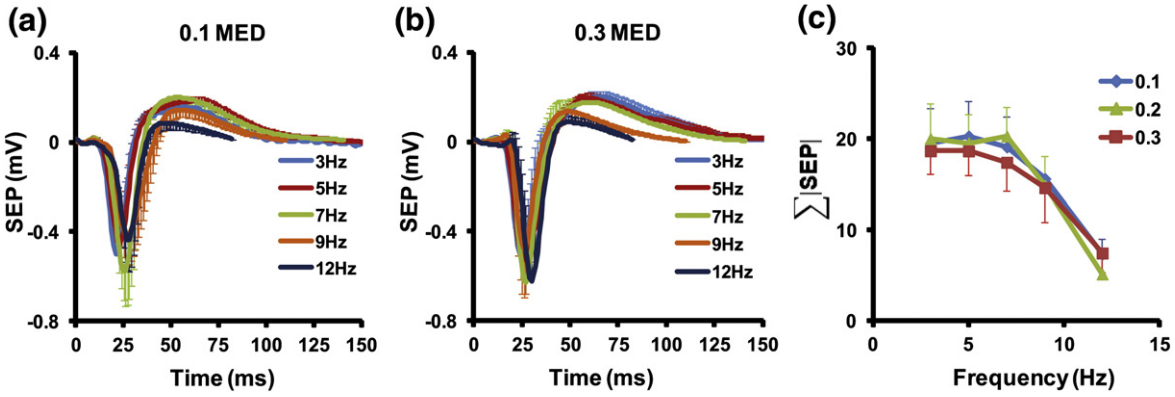

Fig. 1. Stimulus frequency dependence of SEP under different levels of medetomidine. (a) Averaged SEPs from the left S1FL following forepaw electrical stimulation of 3, 5, 7, 9 and 12 Hz at 0.1 mg/kg/h medetomidine. (b) Averaged SEPs from the left SIFL following forepaw electrical stimulation at 0.3 mg/kg/h medetomidine. (c) The integral of SEP amplitude versus the stimulus frequency at the three dosages of medetomidine, 0.1, 0.2, and 0.3 mg/kg/h. Error bar represents SEM and n = 8 for each dose.

highest at 0.2, then 0.3 and lowest at 0.1 mg/kg/h dose of medetomidine ($p < 0.05$). However, the integral of amplitude was not significantly different: 15.0 ± 2.5 at 0.1 (mean ± SEM; n = 8), 14.0 ± 2.7 at 0.2, and 13.9 ± 2.0 at 0.3. Especially, linear relationship between the average BOLD signal change and integral of SEP amplitude was found (Fig. 2c) and there was no difference between dosages of medetomidine. This indicates that the neurovascular coupling under the three dosages of medetomidine remains the same.

Resting BOLD and EEG under medetomidine

Results comparing the resting-state BOLD signal and that of EEG under the same condition are summarized in Fig. 3. Fig. 3a shows representative BOLD time-courses from the left S1FL under the three dosages of medetomidine. No suppression of signal change is apparent which is further supported by the unchanged total power (Fig. 3b). A similar activity was seen in the resting EEG where amplitudes of the basal neural activity (Fig. 3d). The total power was 0.022 ± 0.0036 (mean ± SEM; n = 8) at 0.1, 0.016 ± 0.0012 at 0.2, and 0.016 ± 0.0026 at 0.3 mg/kg/h medetomidine (Fig. 3e). Although the EEG power at 0.1 mg/kg/h was slightly higher, there was no significance between the 0.1 and 0.2 medetomidine groups ($p > 0.1$) neither between the 0.1 and 0.3 medetomidine groups ($p > 0.39$). Therefore, although there was slightly higher EEG power in the 0.1 medetomidine group, it may not be large enough to be reflected in BOLD signal. We then analyzed the coherence of BOLD signals between the left and right S1FLs (Fig. 3c). The inter-hemispheric BOLD signal coherence decreased at higher dosage of medetomidine in all frequency investigated ($p < 0.01$). On the other hand, inter-hemispheric EEG coherence was mostly unchanged by medetomidine, except in the gamma band (Fig. 3f). Significant reduction of gamma band coherence was detected at 0.3 mg/kg/h medetomidine ($p < 0.05$).

Comparison with isoflurane

Respiration rate, respiration flow, and respiration pressure were adjusted to maintain arterial blood pH at 7.4 ± 0.05, pCO_2 at 35 ± 0.4 mm Hg, pO_2 at 200 ± 10 mm Hg, and MABP at 110 ± 5 mm Hg under 1% isoflurane. Physiological measures were unchanged under 2% isoflurane: pH at 7.4 ± 0.05, pCO_2 at 33 ± 0.3 mm Hg, pO_2 at 184 ± 9 mm Hg, and MABP at 109 ± 10 mm Hg; and under 3% isoflurane: pH at 7.3 ± 0.04, pCO_2 at 34.5 ± 0.8 mm Hg, pO_2 at 188 ± 7 mm Hg, and MABP at 114 ± 6 mm Hg.

Fig. 4a shows the isoflurane level-dependent BOLD activation in the SIFL areas with 3 mA, 9 Hz stimulation. Highly activated BOLD signal was detected at 1.0% isoflurane with drastic suppression at 2.0% and only very slight activation can be detected at 3.0% isoflurane. A similar trend was observed in the SEP though the activation was almost abolished at 3.0% isoflurane (Fig. 4b). High correlation between BOLD and SEP is further illustrated in Fig. 4c where a linear trend can be seen.

The resting-state synchrony of the BOLD and EEG signals between the left and right SIFLs is depicted in Fig. 5. Contrary to medetomidine, resting-state BOLD signal was suppressed progressively by increasing isoflurane levels (Fig. 5a) with power reduced from 0.33 ± 0.049 to

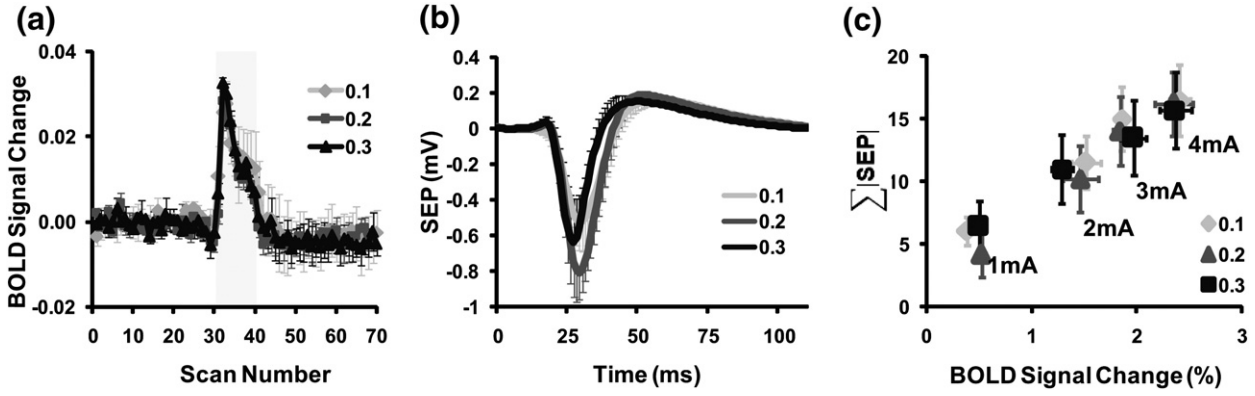

Fig. 2. Correlation between BOLD and SEP under different levels of medetomidine. (a) Averaged time courses of the BOLD response from the left SIFL region following electrical stimulation of 9 Hz and 3 mA at 0.1, 0.2, and 0.3 mg/kg/h medetomidine (n = 5 for each dosage). (b) Averaged SEPs from the left SIFL following the same stimulation at 0.1, 0.2, and 0.3 mg/kg/h medetomidine (n = 8 for each dosage). (c) The relationship between the BOLD activation signal change and the SEP response under 9 Hz and 1, 2, 3, and 4 mA stimulation at three dosages of medetomidine. Error bar represents SEM.

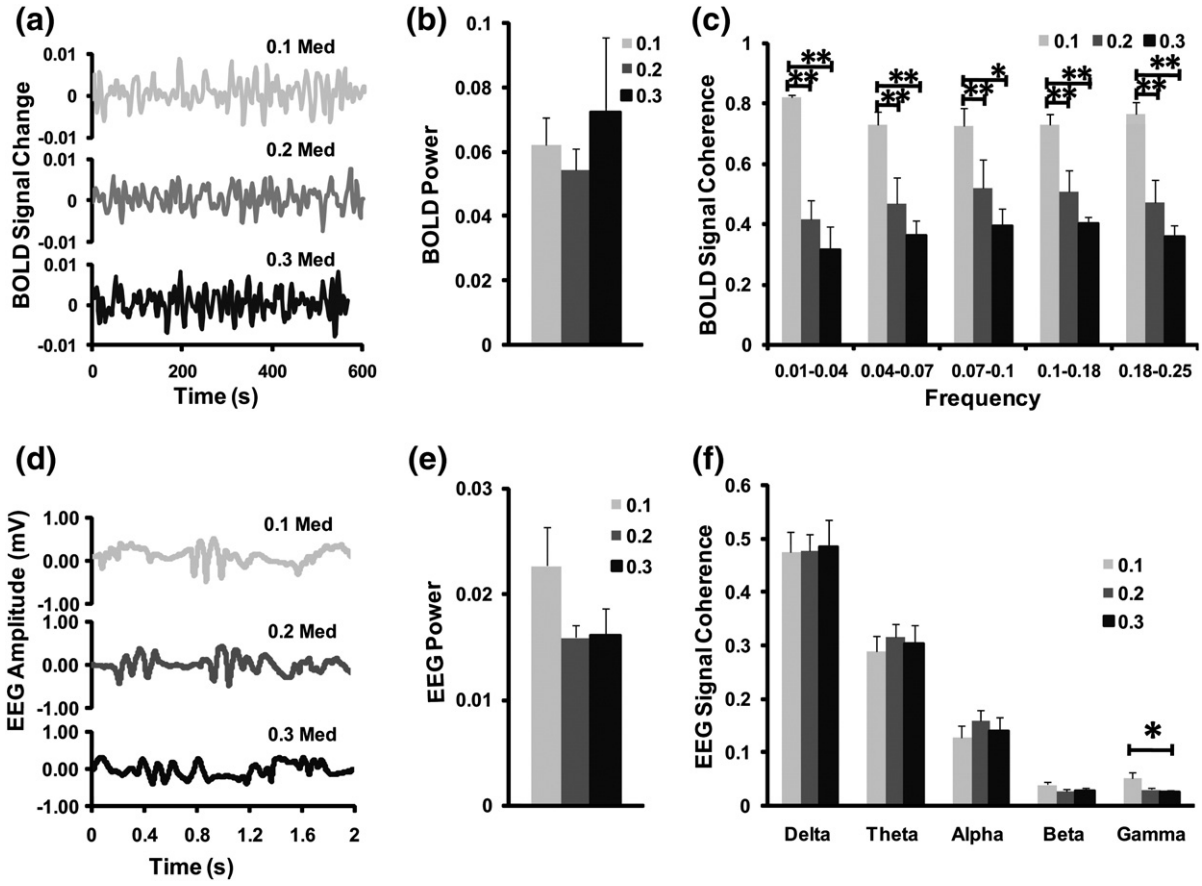

Fig. 3. Resting-state BOLD and EEG in SIFL under medetomidine. (a) Representative resting-state BOLD signals from left SIFL showing no change in amplitude under each of the medetomidine dosages tested, 0.1, 0.2 and 0.3 mg/kg/h. (b) Average total power shows no difference with medetomidine dosage ($n = 5$ for each dosage). (c) Coherence of resting BOLD signal between left and right SIFLS in various frequency bands within 0.01 to 0.25 Hz. (d) Representative resting EEG signals from rats at each of the medetomidine dosages. (e) Total power of EEG signal from the average of left and right SIFLs shows no change at different dosages of medetomidine ($n = 8$ for each dosage). (f) EEG signal coherence between the left and right SIFLs at different frequency bands. Error-bar represents SEM and asterisks represent significance where *: $p < 0.05$; **: $p < 0.01$.

0.19 ± 0.02, and 0.047 ± 0.012 at 1.0%, 2.0% and 3.0% isoflurane, respectively (Fig. 5b). The correlation between the left and right SIFLs was significantly reduced from 0.70 ± 0.024 at 1.0% isoflurane, to 0.57 ± 0.022 at 2.0% ($p < 0.01$) and to 0.36 ± 0.025 at 3.0% ($p < 0.01$). This is also seen in the inter-hemispheric coherence of the resting BOLD signal showing significant suppression across all frequency bands (Fig. 5c). The resting EEG under the same conditions shows large change with bursting activity at 2.0% isoflurane, and with most activity suppressed at 3.0% (Fig. 5d). This is also reflected as dramatic decrease in EEG power at higher isoflurane levels (Fig. 5e). The suppression of resting neural activity is evident in all frequency bands from 1.0% to 2.0% (except beta and gamma bands) and from 2.0% to 3.0% isoflurane (Fig. 5f).

Discussion

Tight coupling was found between the EEG and BOLD signals recorded from the rat somatosensory cortex under various doses of medetomidine

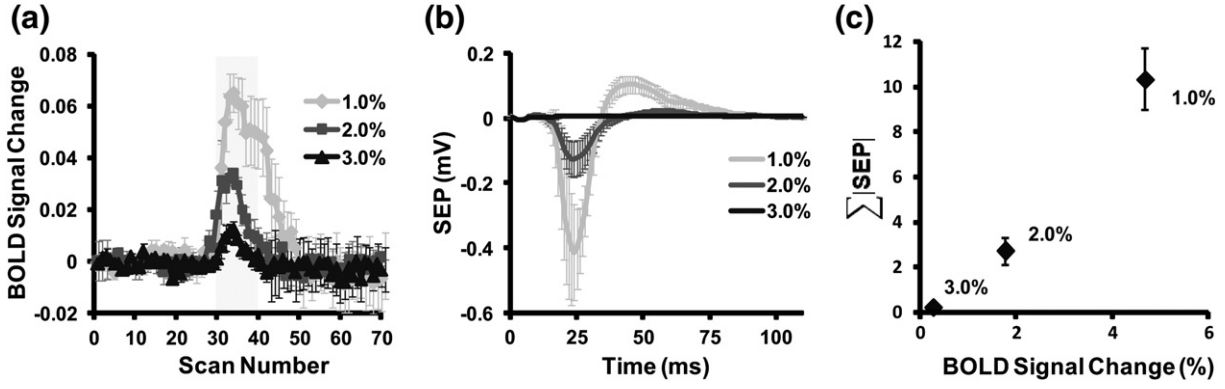

Fig. 4. Stimulus evoked BOLD and SEP under isoflurane. (a) Averaged time courses of BOLD response from the left SIFL region following electrical current stimulation of 9 Hz and 3 mA at 1.0, 2.0, and 3.0% isoflurane ($n = 5$ for each dosage). (b) Averaged SEPs from the left SIFL following the same stimulation at 1.0, 2.0, and 3.0% isoflurane ($n = 6$ for each dosage). (c) Relationship between BOLD activation signal changes and integral of SEP amplitude. Error-bar represents SEM.

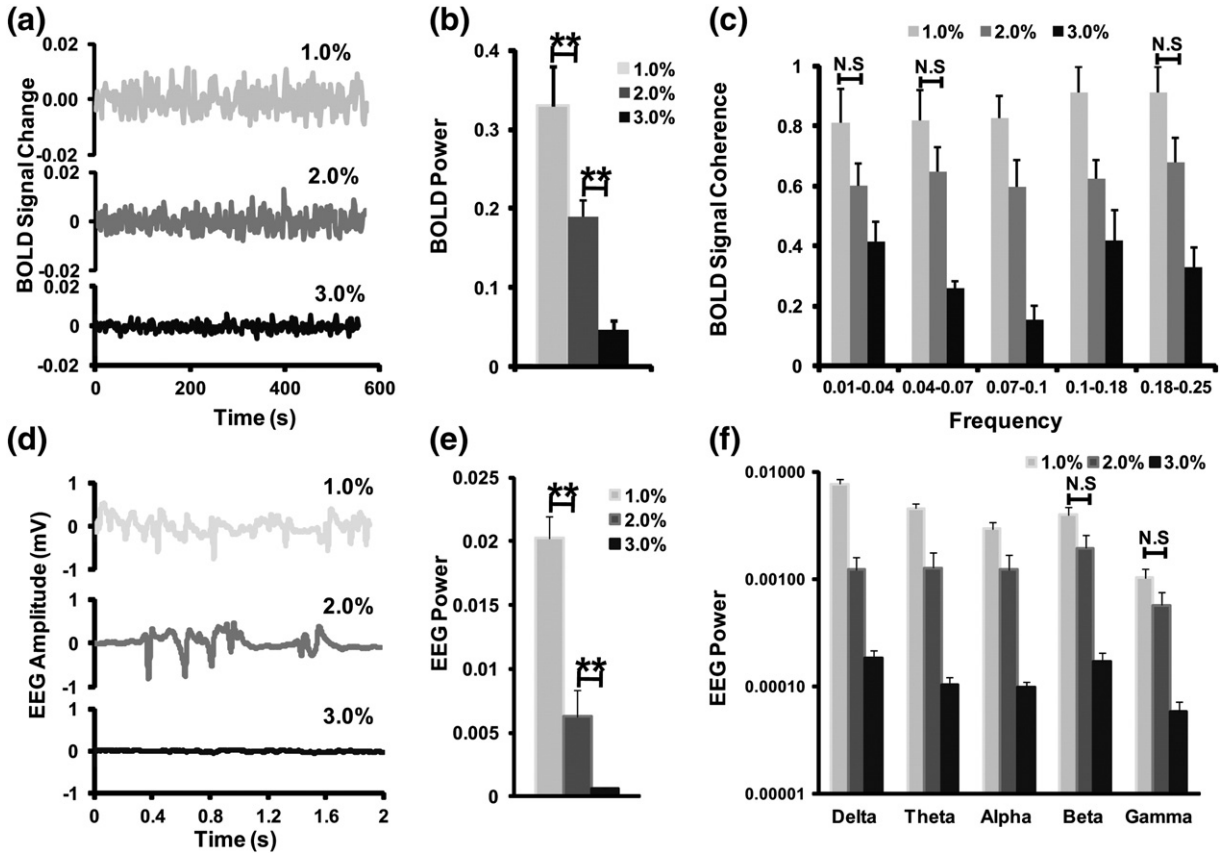

Fig. 5. Resting-state BOLD and EEG signals in SIFL under isoflurane. (a) Representative time course of BOLD signal from the left SIFL of one rat under the isoflurane levels tested: 1.0, 2.0 and 3.0%. (b) Average total power decreased significantly with increasing isoflurane levels (n = 5 for each dosage). (c) BOLD signal coherence between left and right SIFLs at different frequency bands shows significant reduction with increased isoflurane level except those marked by N.S. (d) Representative resting EEG signals from one rat at each of the isoflurane levels. (e) Total power of EEG signal from the left and right SIFL regions was suppressed by increasing dosages of isoflurane (n = 6 for each dosage). (f) Power distribution of resting EEG reveals suppression of neural activity in all frequency bands with increased isoflurane levels where significant difference is seen in all the groups except those marked by N.S.

sedation or isoflurane anesthesia. Although medetomidine reduces CBF and isoflurane increases CBF dose dependently, the linear EEG–BOLD correlations suggest that the stimulus evoked and resting-state hemodynamic fluctuations observed are representative of neural activity rather than non-neuronal phenomena. Especially, this study confirmed our previous finding that medetomidine suppresses functional connectivity but not evoked activation in the somatosensory areas. The EEG study further revealed that gamma coherence between bilateral SIFL was decreased similarly to the resting BOLD correlation under high dose of medetomidine. This suggests that gamma synchrony may underlie the resting-state functional connectivity.

Stimulation-induced BOLD and SEP under medetomidine

Since medetomidine is a vasoconstrictor that can alter CBF in a dosage dependent way, there is concern whether the neurovascular coupling is also changed. We showed that stimulus current dependence of BOLD and SEP under medetomidine sedation does not change with increased dosage (Fig. 2). Although linear relationship between BOLD and SEP could be seen with varying stimulus intensity, the relationship in terms of stimulus frequency is not linear. From our previous study (Nasrallah et al., 2012), a stimulus ~9 Hz elicited maximum BOLD response in SI under medetomidine which is consistent with the literature (Zhao et al., 2008). However, the SEP under the same stimuli revealed an optimal frequency response in the range of 3–7 Hz and decreased at ≥9 Hz (Fig. 1c). Similar discrepancy in the frequency dependent response between hemodynamics and SEP has also been reported under isoflurane where SEP shows high amplitude at low stimulus frequency but hemodynamic response is low (Masamoto et al., 2007). Despite that, both BOLD and SEP didn't show medetomidine dosage dependency with no significant difference between 0.3 and 0.1 mg/kg/h. These together indicate that BOLD and SEP are tightly coupled and the neurovascular coupling is not affected by medetomidine in the dosages used.

Neural correlates of spontaneous hemodynamic synchrony under medetomidine

In this study, we found that suppression of inter-hemispheric BOLD synchrony under medetomidine corresponded to a gradual decrease in EEG gamma band coherence (Fig. 3f). A number of studies have investigated the neural correlates of spontaneous hemodynamic correlation in different species and brain states. In somatosensory area in rodent, the δ band power was correlated with reduced resting BOLD synchrony as the depth of α-chloralose increased (Lu et al., 2007). A decrease in gamma power with increasing levels of isoflurane was reported but the correlation in δ and θ bands was more representative of the BOLD correlation (Pan et al., 2011). Therefore correlation with particular band limited power may be anesthesia dependent. In the monkey, BOLD fluctuations and low frequency modulation of gamma power in visual cortex under isoflurane (Shmuel and Leopold, 2008) and remifentanil (Magri et al., 2012) anesthesia were observed. A tight coupling of gamma power in cortex with global fluctuation in monkey brain was reported (Schölvinck et al., 2010) which was also observed in the human auditory system (Nir et al., 2008). Furthermore, with its task-dependent suppression in posterior cingulate and medial prefrontal cortex, gamma-band activity has also been suggested to be a putative neural

underpinning of the default mode network (Jerbi et al., 2010). The behavioral significance and physiological functions of gamma synchrony are not well understood but growing evidence has linked these oscillations with high level cognitive processing (Herrmann et al., 2004; Kaiser and Lutzenberger, 2003) as a mechanism for maintaining coherent interactions among distributed functional areas (Engel et al., 1997). Synchronized gamma rhythms have been related to consciousness (Engel and Singer, 2001), attention and memory (Fries et al., 2007). The neuronal link of gamma oscillations was emphasized by Gray and Singer (1989) who showed that action potentials generated by cortical cells align with the oscillatory rhythm in the beta and gamma range. Accumulating evidence reporting the tight coupling between the BOLD signal and gamma-band neuronal activity may be a key to bridging the gap between functional MRI and its neuronal underpinnings (Lachaux et al., 2007; Mukamel et al., 2005; Nir et al., 2007; Shmuel et al., 2006).

How gamma oscillations can be a key to linking the resting BOLD signal to neural connectivity? GABAergic neurons play a crucial role in the generation of high-frequency oscillations and local synchronization (Bartos et al., 2007; Draguhn et al., 1998; Nase et al., 2003) while glutamatergic connections appear to control their long range synchronization (Fisahn et al., 2004; Traub et al., 2005) and neurotransmitter levels. This is supported by a study showing that glutamate correlated positively and GABA correlated negatively with functional connectivity in the default mode network (Kapogiannis et al., 2013). Another study suggests that high correlation between the hemodynamic response and the gamma oscillation during visual stimulation reflects neuronal synchronization of inhibitory interneurons (Niessing et al., 2005). Additionally, cholinergic modulation of gamma oscillations has also been reported where cholinergic antagonists enhanced gamma oscillations (Rodriguez et al., 2004; Wespatat et al., 2004). Our study suggests another possibility with a neuromodulator, the α2 adrenergic system. In fact, the influence of α2 adrenergic receptors on cortical and subcortical neural oscillation has been well recognized (Buzsáki et al., 1991). Therefore, α2 adrenergic system could also play an important role in functional connectivity.

Current theory on anesthesia and consciousness suggests that the disruption of cortical integration, especially long-range cortico-cortical and feedback interactions, can be an important mechanism of the loss of consciousness (Alkire et al., 2008). The unchanged somatosensory activity but disrupted connectivity between cortical areas under medetomidine may explain the mechanism of the sedative effect that the animal remained conscious of the sensory input but not able to react. Considering the essential role of gamma oscillation in sensory integration, the reduced gamma rhythms and functional connectivity may be related to the altered consciousness, attention, awareness and information processing under medetomidine sedation.

An intriguing question is how a low power component like gamma band could contribute to large change in BOLD coherence. In our study, change in the coherence of BOLD signal and gamma oscillation was not accompanied by change in their power though a slight but insignificant decrease of EEG power (~16.4%) from 0.1 to 0.2 mg/kg/h medetomidine was observed. Compared to the EEG and BOLD power change under isoflurane, where 53.8% reduction of EEG power from 1% to 2% isoflurane corresponded to only 26.9% decrease of BOLD power, the slightly higher EEG power in the 0.1 medetomidine group may not be large enough to be reflected in the BOLD signal amplitude but amplitude-independent measure such as coherence would still be detectable. BOLD signal change is highly correlated with local field potential and can include contribution from all the frequency bands (Bruyns-Haylett et al., in press). So far, there is no study looking at the proportional contribution of EEG band limited power to the BOLD signal change, and hence will be an important area in the future research.

Isoflurane suppresses neural activity and connectivity

It is evident that the type of anesthetic used could significantly affect spontaneous brain activity while making it more difficult to delineate their neural origin. The specific effect of medetomidine on connectivity can be further understood by comparing with isoflurane, which is known to suppress brain activity (Masamoto et al., 2007, 2009). Opposed to medetomidine, a strong anesthesia level dependent reduction of the somatosensory activation was observed from 1% to 3% isoflurane. BOLD activation was largely suppressed and the evoked potential reached nearly zero at 3% isoflurane. Not only the evoked response, but also the resting activity was also dramatically suppressed. The resting EEG power was minimal at 3% isoflurane and this suppression was global to all frequency especially in the δ, θ, and α bands even at 2% isoflurane. Therefore, the reduced resting BOLD correlation under higher isoflurane level simply reflects a global suppression of all kinds of neural activity rather than a specific suppression of synchrony like those shown in the medetomidine study. Similar suppression of spontaneous CBF/BOLD fluctuations under isoflurane anesthesia that correlated with suppression in neural activity was also reported (Liu et al., 2011). In our analysis, we also observed large reduction of EEG spectral power under higher isoflurane levels but the coherence was high in all frequency bands and didn't reflect the dosage dependent change. This may be because the EEG bursting at 2% isoflurane which rends the whole brain highly synchronized, and the nearly abolished EEG at 3% isoflurane made the coherence calculation becomes artifactually high.

Interestingly, even when most neural activity was suppressed at 3.0% isoflurane, certain level of BOLD activation and resting correlation can still be observed. The unexpected BOLD activation 3.0% may be due to the particular neurovascular coupling at the stimulus frequency used. A study on neurovascular coupling at different isoflurane levels showed that while SEPs of different stimulus frequencies all decrease with increased isoflurane, the evoked CBF response decreases only at high frequency and increases for stimulus interval >100 ms (<10 Hz) (Masamoto et al., 2007, 2009). Therefore, the BOLD response at the 9 Hz stimulation used in this study would not decrease as drastic as SEP. This may also partly explain high resting BOLD correlation at 3.0% isoflurane. Alternatively, this residual correlation at 3.0% isoflurane may be due to correlated noise in the BOLD signal such as physiological noise.

Conclusion

The tight and unaffected neurovascular coupling observed between evoked potential and BOLD activation under medetomidine sedation suggests that the spontaneous BOLD fluctuations may reflect altered neural oscillation, especially in the gamma band. This supports the neuronal origin of functional connectivity measured by fMRI. Further study, especially using concurrent measurement of BOLD and electrophysiology, will be needed to understand the link with gamma synchrony. Unlike medetomidine, isoflurane suppresses both evoked and resting cortical neural activities. The particular reduction of neural oscillation provides another insight to the differential mechanism behind medetomidine sedation compared to other anesthetics.

Acknowledgments

The work was supported by the Intramural Research Program of the Singapore Bioimaging Consortium, Biomedical Sciences Institutes, Agency for Science, Technology and Research (A*STAR), Singapore.

References

Adamczak, J., Farr, T., Seehafer, J., Kalthoff, D., Hoehn, M., 2010. High field BOLD response to forepaw stimulation in the mouse. NeuroImage 51, 704–712.
Alkire, M., Hudetz, A., Tononi, G., 2008. Consciousness and anesthesia. Science 322, 876.
Antognini, J.F., Carstens, E., 1999. Isoflurane blunts electroencephalographic and thalamic–reticular formation responses to noxious stimulation in goats. Anesthesiology 91, 1770.
Bartos, M., Vida, I., Jonas, P., 2007. Synaptic mechanisms of synchronized gamma oscillations in inhibitory interneuron networks. Nat. Rev. Neurosci. 8, 45–56.
Biswal, B., Yetkin, F., Haughton, V., Hyde, J., 1995. Functional connectivity in the motor cortex of resting human brain using echo-planar MRI. Magn. Reson. Med. 34, 537–541.

Bruyns-Haylett, M., Harris, S., Boorman, L., Zheng, Y., Berwick, J., Jones, M., 2013. The resting-state neurovascular coupling relationship: rapid changes in spontaneous neural activity in the somatosensory cortex are associated with haemodynamic fluctuations that resemble stimulus-evoked haemodynamics. Eur. J. Neurosci. http://dx.doi.org/10.1111/ejn.12295 (in press, published online: 10 JUL 2013).
Buzsáki, G., Kennedy, B., Solt, V.B., Ziegler, M., 1991. Noradrenergic control of thalamic oscillation: the role of α-2 receptors. Eur. J. Neurosci. 3, 222–229.
Chuang, K., van Gelderen, P., Merkle, H., Bodurka, J., Ikonomidou, V., Koretsky, A., Duyn, J., Talagala, S., 2008. Mapping resting-state functional connectivity using perfusion MRI. NeuroImage 40, 1595–1605.
Draguhn, A., Traub, R.D., Schmitz, D., Jefferys, J., 1998. Electrical coupling underlies high-frequency oscillations in the hippocampus in vitro. Nature 394, 189–192.
Engel, A., Singer, W., 2001. Temporal binding and the neural correlates of sensory awareness. Trends Cogn. Sci. 5, 16–25.
Engel, A., Roelfsema, P., Fries, P., Brecht, M., Singer, W., 1997. Role of the temporal domain for response selection and perceptual binding. Cereb. Cortex 7, 571–582.
Fisahn, A., Contractor, A., Traub, R., Buhl, E., Heinemann, S., McBain, C., 2004. Distinct roles for the kainate receptor subunits GluR5 and GluR6 in kainate-induced hippocampal gamma oscillations. J. Neurosci. 24, 9658–9668.
Fries, P., Nikoli, D., Singer, W., 2007. The gamma cycle. Trends Neurosci. 30, 309–316.
Goldman, R., Stern, J., Engel, J., Cohen, M., 2002. Simultaneous EEG and fMRI of the alpha rhythm. NeuroReport 13, 2487–2492.
Gray, C., Singer, W., 1989. Stimulus-specific neuronal oscillations in orientation columns of cat visual cortex. Proc. Natl. Acad. Sci. U. S. A. 86, 1698–1702.
He, B., Snyder, A., Zempel, J., Smyth, M., Raichle, M., 2008. Electrophysiological correlates of the brain's intrinsic large-scale functional architecture. Proc. Natl. Acad. Sci. U. S. A. 105, 16039–16044.
Herrmann, C., Munk, M., Engel, A., 2004. Cognitive functions of gamma-band activity: memory match and utilization. Trends Cogn. Sci. 8, 347–355.
Jerbi, K., Vidal, J., Ossandon, T., Dalal, S., Jung, J., Hoffmann, D., Minotti, L., Bertrand, O., Kahane, P., Lachaux, J., 2010. Exploring the electrophysiological correlates of the default-mode network with intracerebral EEG. Front. Syst. Neurosci. 4, 27.
Kaiser, J., Lutzenberger, W., 2003. Induced gamma-band activity and human brain function. Neuroscientist 9, 475–484.
Kapogiannis, D., Reiter, D., Willette, A., Mattson, M., 2013. Posteromedial cortex glutamate and GABA predict intrinsic functional connectivity of the default mode network. NeuroImage 64, 112–119.
Lachaux, J., Fonlupt, P., Kahane, P., Minotti, L., Hoffmann, D., Bertrand, O., Baciu, M., 2007. Relationship between task-related gamma oscillations and BOLD signal: new insights from combined fMRI and intracranial EEG. Hum. Brain Mapp. 28, 1368–1375.
Larson, C., Davidson, R., Abercrombie, H., Ward, R., Schaefer, S., Jackson, D., Holden, J., Perlman, S., 1998. Relations between PET-derived measures of thalamic glucose metabolism and EEG alpha power. Psychophysiology 35, 162–169.
Laufs, H., Kleinschmidt, A., Beyerle, A., Eger, E., Salek-Haddadi, A., Preibisch, C., Krakow, K., 2003a. EEG-correlated fMRI of human alpha activity. NeuroImage 19, 1463–1476.
Laufs, H., Krakow, K., Sterzer, P., Eger, E., Beyerle, A., Salek-Haddadi, A., Kleinschmidt, A., 2003b. Electroencephalographic signatures of attentional and cognitive default modes in spontaneous brain activity fluctuations at rest. Proc. Natl. Acad. Sci. U. S. A. 100, 11053–11058.
Leopold, D., Logothetis, N., 2003. Spatial patterns of spontaneous local field activity in the monkey visual cortex. Rev. Neurosci. 14, 195–205.
Lin, C., 1994. Uptake of anaesthetic gases and vapours. Anaesth. Intensive Care 22, 363–373.
Lindgren, K., Larson, C., Schaefer, S., Abercrombie, H., Ward, R., Oakes, T., Holden, J., Perlman, S., Benca, R., Davidson, R., 1999. Thalamic metabolic rate predicts EEG alpha power in healthy control subjects but not in depressed patients. Biol. Psychiatry 45, 943–952.
Liu, X., Zhu, X., Zhang, Y., Chen, W., 2011. Neural origin of spontaneous hemodynamic fluctuations in rats under burst-suppression anesthesia condition. Cereb. Cortex 21, 374–384.
Lu, H., Zuo, Y., Gu, H., Waltz, J., Zhan, W., Scholl, C., Rea, W., Yang, Y., Stein, E., 2007. Synchronized delta oscillations correlate with the resting-state functional MRI signal. Proc. Natl. Acad. Sci. U. S. A. 104, 18265–18269.
Magri, C., Schridde, U., Murayama, Y., Panzeri, S., Logothetis, N., 2012. The amplitude and timing of the BOLD signal reflects the relationship between local field potential power at different frequencies. J. Neurosci. 32, 1395–1407.
Masamoto, K., Kanno, I., 2012. Anesthesia and the quantitative evaluation of neurovascular coupling. J. Cereb. Blood Flow Metab. 32, 1233–1247.
Masamoto, K., Kim, T., Fukuda, M., Wang, P., Kim, S., 2007. Relationship between neural, vascular, and BOLD signals in isoflurane-anesthetized rat somatosensory cortex. Cereb. Cortex 17, 942–950.
Masamoto, K., Fukuda, M., Vazquez, A., Kim, S., 2009. Dose-dependent effect of isoflurane on neurovascular coupling in rat cerebral cortex. Eur. J. Neurosci. 30, 242–250.
Michels, L., Bucher, K., Lüchinger, R., Klaver, P., Martin, E., Jeanmonod, D., Brandeis, D., 2010. Simultaneous EEG–fMRI during a working memory task: modulations in low and high frequency bands. PLoS One 5 (e10298–e10298).
Moosmann, M., Ritter, P., Krastel, I., Brink, A., Thees, S., Blankenburg, F., Taskin, B., Obrig, H., Villringer, A., 2003. Correlates of alpha rhythm in functional magnetic resonance imaging and near infrared spectroscopy. NeuroImage 20, 145–158.
Mukamel, R., Gelbard, H., Arieli, A., Hasson, U., Fried, I., Malach, R., 2005. Coupling between neuronal firing, field potentials, and fMRI in human auditory cortex. Science 309, 951–954.
Nase, G., Singer, W., Monyer, H., Engel, A., 2003. Features of neuronal synchrony in mouse visual cortex. J. Neurophysiol. 90, 1115–1123.
Nasrallah, F., Tan, J., Chuang, K., 2012. Pharmacological modulation of functional connectivity: alpha-2-adrenergic receptor agonist alters synchrony but not neural activation. NeuroImage 60, 436–446.
Niessing, J., Ebisch, B., Schmidt, K., Niessing, M., Singer, W., Galuske, R., 2005. Hemodynamic signals correlate tightly with synchronized gamma oscillations. Science 309, 948–951.
Nir, Y., Fisch, L., Mukamel, R., Gelbard-Sagiv, H., Arieli, A., Fried, I., Malach, R., 2007. Coupling between Neuronal firing rate, gamma LFP, and BOLD fMRI is related to interneuronal correlations. Curr. Biol. 17, 1275–1285.
Nir, Y., Mukamel, R., Dinstein, I., Privman, E., Harel, M., Fisch, L., Gelbard-Sagiv, H., Kipervasser, S., Andelman, F., Neufeld, M., Kramer, U., Arieli, A., Fried, I., Malach, R., 2008. Interhemispheric correlations of slow spontaneous neuronal fluctuations revealed in human sensory cortex. Nat. Neurosci. 11, 1100–1108.
Pan, W., Thompson, G., Magnuson, M., Majeed, W., Jaeger, D., Keilholz, S., 2011. Broadband local field potentials correlate with spontaneous fluctuations in functional magnetic resonance imaging signals in the rat somatosensory cortex under isoflurane anesthesia. Brain Connect. 1, 119–131.
Pawela, C., Biswal, B., Hudetz, A., Schulte, M., Li, R., Jones, S., Cho, Y., Matloub, H., Hyde, J., 2009. A protocol for use of medetomidine anesthesia in rats for extended studies using task-induced BOLD contrast and resting-state functional connectivity. NeuroImage 46, 1137–1147.
Paxinos, G., Watson, C., 1995. The Rat Nervous System, 2nd edition. Academic Press, San Diego.
Rodriguez, R., Kallenbach, U., Singer, W., Munk, M.H., 2004. Short- and long-term effects of cholinergic modulation on gamma oscillations and response synchronization in the visual cortex. J. Neurosci. 24, 10369–10378.
Scheeringa, R., Petersson, K., Kleinschmidt, A., Jenson, O., Bastiaansen, M., 2012. EEG alpha power modulation of fMRI resting-state connectivity. Brain Connect. 2, 254–264.
Schölvinck, M., Maier, A., Ye, F., Duyn, J., Leopold, D., 2010. Neural basis of global resting-state fMRI activity. Proc. Natl. Acad. Sci. U. S. A. 107, 10238–10243.
Shmuel, A., Leopold, D., 2008. Neuronal correlates of spontaneous fluctuations in fMRI signals in monkey visual cortex: implications for functional connectivity at rest. Hum. Brain Mapp. 29, 751–761.
Shmuel, A., Augath, M., Oeltermann, A., Logothetis, N., 2006. Negative functional MRI response correlates with decreases in neuronal activity in monkey visual area V1. Nat. Neurosci. 9, 569–577.
Tagliazucchi, E., von Wegner, F., Morzelewski, A., Borisov, S., Jahnke, K., Laufs, H., 2012. Automatic sleep staging using fMRI functional connectivity data. NeuroImage 63, 63–72.
Traub, R., Bibbig, A., LeBeau, F., Cunningham, M., Whittington, M., 2005. Persistent gamma oscillations in superficial layers of rat auditory neocortex: experiment and model. J. Physiol. 562, 3–8.
Weber, R., Ramos, C.P., Wiedermann, D., van Camp, N., Hoehn, M., 2006. A fully noninvasive and robust experimental protocol for longitudinal fMRI studies in the rat. NeuroImage 29, 1303–1310.
Wespatat, V., Tennigkeit, F., Singer, W., 2004. Phase sensitivity of synaptic modifications in oscillating cells of rat visual cortex. J. Neurosci. 24, 9067–9075.
Zhao, F., Zhao, T., Zhou, L., Wu, Q., Hu, X., 2008. BOLD study of stimulation-induced neural activity and resting-state connectivity in medetomidine-sedated rat. NeuroImage 39, 248–260.